Copyright © 2017 ABCM

Analytical and Numerical Model of a Cold Rolling Process

De Aguiar, João B., joao.aguiar@ufabc.edu.br[1]
De Aguiar, José M., josemaguiar@gmail.com[2]

[1] Universidade Federal do ABC, Av. dos Estados, 5001, Santa Terezinha, Santo André, SP, Brasil
[2] Faculdade de Tecnologia de São Paulo, FATEC-SP, Praça Cor. Fernando Prestes, 30, Bom Retiro, São Paulo, SP, Brasil

Abstract. *Rolling process is a quite important conforming method, being the principal in the manufacturing industry. In this work analytical and numerical approaches are used to understand the mechanics of the problem. Main equations for equilibrium as the material is rolled are presented. Elasto-plastic constitutive behavior with hardening is supposed. Frictional contact at the moving interface is considered. A classical analytical solution for a plane case is reviewed. For the same problem a numerical procedure, based on a finite element scheme is presented. Results obtained from the numerical simulation are used to verify hypotheses in the analytical procedure. Process parameters such as feed velocity, friction and roll velocity are used to verify the final form and stress field.*

Keywords: *rolling, numerical model, analytical formula, parameter effects, comparisons*

1. INTRODUCTION

Rolling process may be defined as a fabrication process in which cross sections of workpieces have their thicknesses reduced, (Kalpakjian & al, 2016). In the development of the process, the workpiece has its sectional area decreased at the same time as its length is augmented. Movement of workpiece is provided by the motion of a set of rolls. Configuration changes are introduced in one or many stages, caused by frictional contact forces with the rolls. In the process large amounts of compression are introduced in the workpiece. These are the most common identifications tags associated with the process.

The workpiece itself may have different thicknesses. Accordingly, it is classified as plate, sheet or ingots. Materials used are many, but use of metals is most common. Behavior is inelastic, with large elasto-plastic stresses being generated. According to the temperature of processing, visco-plastic behavior, dependent on temperature and rate, is encountered in practice. At high temperatures - hot rolling - analysis of the process couples mechanical and thermal effects (Shahani et al, 2009). At lower temperatures, an elasto-plastic analysis suffices in the estimation of the forces, stresses and strains in the process. In this work this case is going to be considered, as a form of verifying the mechanics of the process.

2. MECHANICAL MODEL

Cold rolling a metal part is a multi-physics problem. Under the mechanical view point only, it requires simultaneous updating of geometry, of the properties of the material as well as the determination of contact forces at the interface between workpiece and roll. Therefore, it is most suitable to solution via numerical procedures. For mechanical problems using finite element procedures, many alternatives exist. Here, Lagrange view point, with continuous updating of configurations, will be chosen. Solution itself may be implicit or explicit. Last procedure being faster, but requiring small increments, will be used.

Disregarding temperature effects and interface lubrication simplifies the treatment to the problem. Introduction of the contact elements, under a penalty approach, requires iterations to be handled separately from main field equations, concatenated with the incremental procedure. Many contact models may be considered. Simplest one considers Coulomb elements, without rate and directionality (Belytschko et all, 2010).

A classical analytical solution will be revisited in order to verify the procedure, its hypotheses and restrictions. The approximate linear form of this solution will be considered for comparison (Backofen, 1972), mostly because it is practical and of simple use. Some additional solutions exist, however, but they resort to numerical schemes relative to the solution of first order differential equations. It makes them less attractive when it comes to estimate results, (Li and Kobayashi, 1982) for example.

2.1. Analytical Approach

Equilibrium of elemental slices of workpiece material in the rolling direction leads to the differential equation of rolling. This equation, first developed by von Karman, writes equilibrium in the x-direction, Fig. 1, as:

$$d(\sigma_x y) - 2(p\sin\phi - \tau\cos\phi)dl = 0 \qquad (1)$$

Copyright © 2017 ABCM

It simply states that the increment of axial resultant $n_x = y\sigma_x$ for each slice in the processing zone is equilibrated by contact forces: normal contact pressure p and tangential contact stress τ. In this description, longitudinal stresses σ_x are supposed to be constant along the slice face, of height y. Inertia term, $\rho dV a_x$, where ρ is the mass density, dV is the volume and a_x the x-component of acceleration, is disregarded. Unitary thickness is supposed.

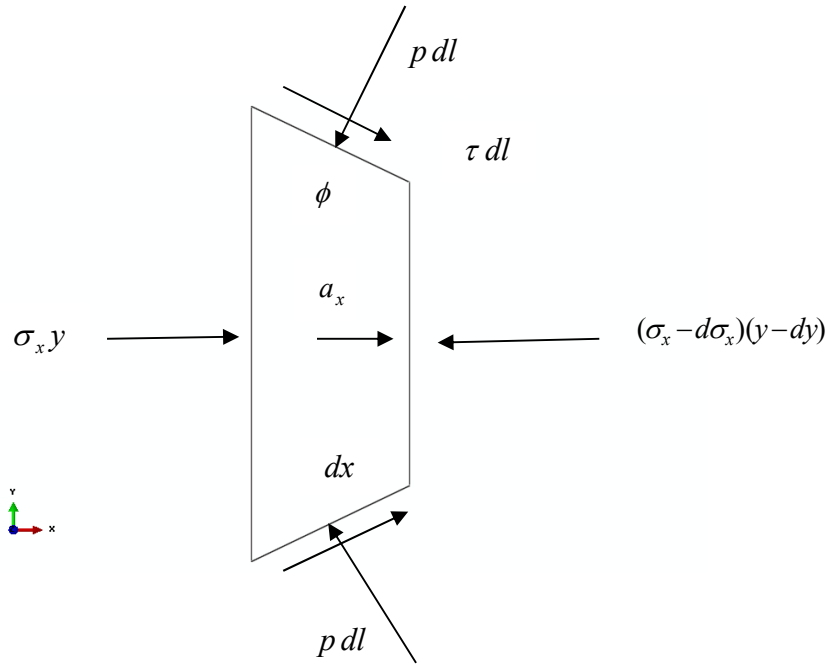

Fig. 1 Horizontal equilibrium of a slice element at the entry zone.

In the same form, equilibrium in the vertical, y direction, Fig. 2, introduces the other stress components:

$$\sigma_y dx - \tau_{xy}\frac{dy}{2} - p\sin\phi dl - \tau\cos\phi dl = 0 \tag{2}$$

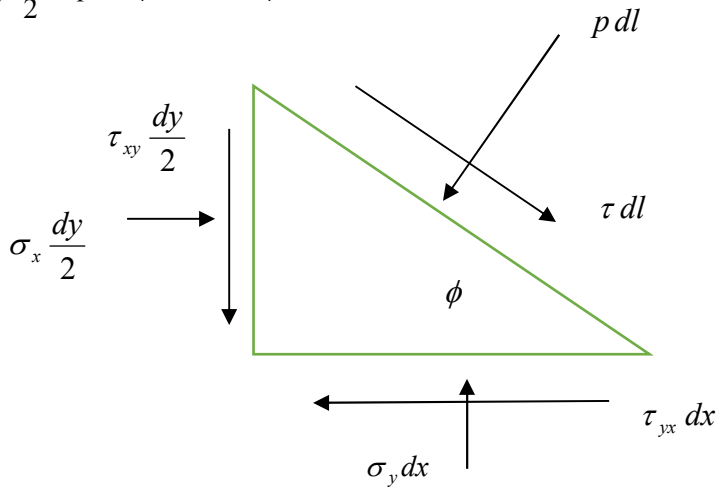

Fog. 2 Vertical equilibrium of wedge element at the entry zone

As shear stresses are supposed small, principal stresses may be approximated by normal components. Under plane strain conditions, Mises criterion ascertains that:

$$\sigma_y - \sigma_x = S_y^{p\varepsilon} \tag{3}$$

Copyright © 2017 ABCM

where $S_y^{P\varepsilon} = 2/\sqrt{3}\, S_y$ is the plane strain yield stress of the material, a multiple of the yield stress S_y. Substitution of Eq. (2) and Eq. (3) into Eq. (1), leads to the differential equation of rolling:

$$\frac{d}{d\phi} p = f(\phi) p + g(\phi) \tag{4}$$

where $\cos\phi = dx/dl$ and $\sin\phi = 0.5dy/dl$. Arch of contact with roll is supposed equal to the hypotenuse of triangle. Assuming Coulomb friction model $\tau = \pm\mu p$, coefficient functions become:

$$f(\phi) = -\frac{\mu \sec\phi}{1 \mp \mu \tan\phi}\left(\frac{2R}{y} + \sec\phi\right) \tag{5}$$

$$g(\phi) = \frac{1}{1 \mp \mu \tan\phi}\left[\frac{2R}{h} S_y^{P\varepsilon} \sin\phi + \frac{d}{d\phi}(S_y^{P\varepsilon})\right] \tag{6}$$

Several numerical methods may be used to get a numerical solution to the above first order differential equation, Eq. (4). A close form solution, however, requires that linearization and approximations be applied. Linearization of the harmonic terms leads to:

$$\frac{d}{d\phi}[y(p - S_y^{P\varepsilon})] \cong 2pR(\phi \pm \mu) \tag{7}$$

Here angle ϕ measures position of the section, with respect to the vertical, measured from the center of the roll of radius R, Fig. 3. The instantaneous slab height is $y = y_f + 2R(1 - \cos\phi)$, being y_f the height at the final, leaving section. The contact pressure p varies with the point of contact, increasing from values at the initial, entry section i-i, angle ϕ_i, up to values at the neutral section n-n, angle ϕ_n decreasing thereafter until the exit region is reached, f-f, angle $\phi_f = 0$.

In the first part, tangential forces help move the workpiece towards the roll gap in the second the reverse occurs. Relative velocities v_r between roll, ωR, and the slab, v, contact elements velocities vary continuously, being zero only at n-n, position of non-slip. Here ω is the rotational velocity of the roll, supposed rigid. Due to the change of direction of frictional forces, the $\pm$ sign is applied to the equations.

During motion, the workpiece of initial width w_i, height y_i and length l_i is pressed against a pair of rolls of radius R, with gap distance y_f at $x = 0$ position. Feed speed v_i is set at the most left section. At the exit section, updated values of these dimensions will have to be obtained, section f-f. If the axial sum $n_{x_y} = yS_y^{P\varepsilon}$ is supposed approximately constant, then Eq. (7) can be integrated to give:

$$p = CS_y^{P\varepsilon} \frac{y}{R} e^{\mp\mu H} \tag{8}$$

where

$$H = 2\sqrt{\frac{2}{y_f}} \tan^{-1}\left(\sqrt{\frac{R}{y_f}}\phi\right) \tag{9}$$

As the arch of contact contains two regions – an entry and an exit zone, friction shows direction changes around the neutral section, where it is zero. Taking the pressure to equal the yield stress at entrance, and to get to zero at exist, determines C and leads to two complementary sentences (Dieter, 1986):

Copyright © 2017 ABCM

$$p = S_y^{P\varepsilon} \frac{y}{y_i} e^{u(H_i - H)} \qquad \phi_i \le \phi \le \phi_n$$
$$p = S_y^{P\varepsilon} \frac{y}{y_f} e^{\mu H} \qquad \phi_n \le \phi \le \phi_f \tag{10}$$

The distribution of pressures on the surface of the roll has a peak value around the neutral point. This distribution depends on the coefficient of friction and the reduction of thickness, $\Delta y = y_i - y_f$. Equating these two sentences renders an approximate value of neutral point angle ϕ_n:

$$\phi_n = \sqrt{\frac{h_e}{R}} \tan\left(\sqrt{\frac{h_e}{R}} \frac{H_n}{2}\right) \tag{11}$$

being $2H_n = H_i + \mu^{-1} \ln(y_i / y_f)$. Integration of the contact forces along the arc of contact between workpiece and the roll surface, gives rise to the roll force components $< R_x, R_y >$ and roll torque M_z:

$$R_x = -\int_{\phi} [-p \sin\phi + \tau \cos\phi] R d\phi \tag{12}$$
$$R_y = -\int_{\phi} [p \cos\phi + \tau \sin\phi] R d\phi \tag{13}$$
$$M_z = -\int_{\phi} \tau R d\phi \tag{14}$$

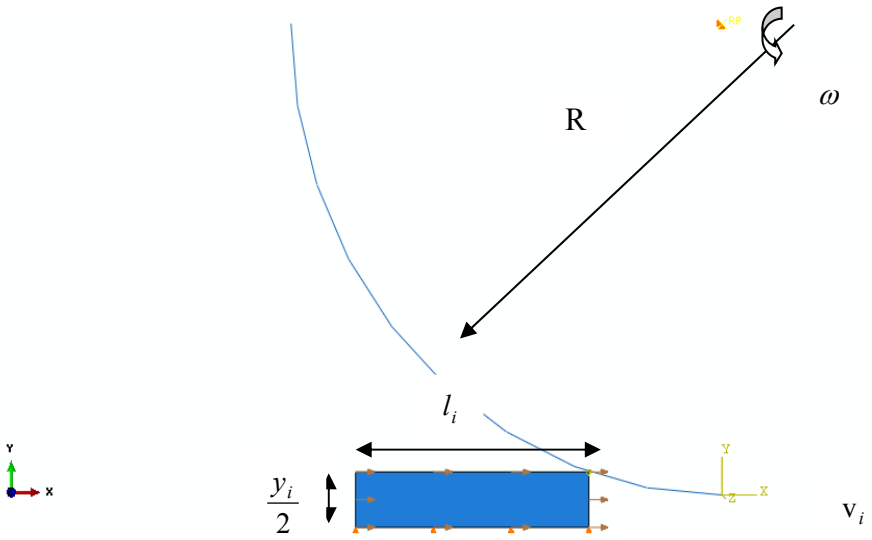

Fig. 3 Initial loading and boundary conditions of the model

2.2. Numerical Approach

The analytical solution above depends on several hypotheses and simplifications that make it restrict. A broader solution may be constructed with an alternative approach to the problem. Finite element method, based on the application of the principle of virtual work, renders an overall, not local, the so-called weak form of equilibrium. Under the stand point of Lagrange, applied in an update manner, this principle equates internal virtual work δW_i

Copyright © 2017 ABCM

$$\delta W_i = \int_{V_{t+\Delta t}} \boldsymbol{\sigma} : \delta \mathbf{e}\, dV_{t+\Delta t} \tag{15}$$

to the external virtual work

$$\delta W_e = \int_{V_{t+\Delta t}} \mathbf{b} \cdot \delta \mathbf{d}\, dV_{t+\Delta t} + \int_{V_{t+\Delta t}} \mathbf{t} \cdot \delta \mathbf{d}\, dS_{t+\Delta t} + \int_{\Gamma_{c\ t+\Delta t}} \mathbf{t}_c \cdot \delta \mathbf{d}_c d\Gamma \tag{16}$$

to set equilibrium between internal stress field $\boldsymbol{\sigma}$ and external tractions $\mathbf{t}$, divided into applied $\mathbf{t}_a$ and contact $\mathbf{t}_c$ tractions and body forces $\mathbf{b}$. Displacement field is denoted by $\mathbf{d}$ whereas $\mathbf{e} = 0.5(\nabla \mathbf{d} + \nabla^T \mathbf{d})$ represents the strains, (Bathe, 1996). In the contact interface, Γ_c, forces and displacements, are factored into normal $< p, d_n >$ and tangential $< \boldsymbol{\tau}, \mathbf{d}_T >$ components.

Present configuration isn't known however. Therefore, the last known configuration known is used as reference for computation of work terms. Use of configuration at time t as reference for the internal virtual work expression requires second Piola-Kirchhoff stresses, denoted as $\mathbf{S}$, energetically conjugated to Green Lagrange strains $\boldsymbol{\varepsilon}$ to substitute the pair $< \boldsymbol{\sigma}, \mathbf{e} >$ in Eq (15). The increment of this work is

$$\partial \delta W_i = \int_{V_t} \partial \mathbf{S} : \delta \boldsymbol{\varepsilon}\, dV_t + \int_{V_t} \mathbf{S} : \partial \delta \boldsymbol{\varepsilon} dV_t \tag{17}.$$

Here the increment of stresses is related to the strains by means of the constitutive equation $\partial \mathbf{S} = \mathbf{C}\boldsymbol{\varepsilon}$, where $\mathbf{C}$ is the constitutive matrix of the material, a tangent matrix. The increments of strain depend on linear and non-linear interpolation terms, $\mathbf{B}$.

Considering the increments, the external virtual work expression, Eq. (16), will appear as:

$$\partial \delta W_{e+c} = \partial \delta W_e + \partial \delta W_c \tag{18}$$

$$\partial \delta W_e = \int_{S_{t+\Delta t}} \partial \mathbf{t}.\delta \mathbf{d}\, I dS_{t+\Delta t} + \int_{S_{t+\Delta t}} \mathbf{t}.\delta \mathbf{d}\, \partial I I^{-1} dS_{t+\Delta t} + \int_{V_{t+\Delta t}} \partial \mathbf{b}.\delta \mathbf{d}\, J dV_{t+\Delta t} + \int_{V_{t+\Delta t}} \mathbf{b}.\delta \mathbf{d}\, \partial J J^{-1} dV_{t+\Delta t} \tag{19}$$

$$\partial \delta W_c = \int_{\Gamma_{t+\Delta t}} \partial \mathbf{t}_c \cdot \delta \mathbf{d} d\Gamma_{t+\Delta t} + \int_{\Gamma_{c\,t+\Delta t}} \mathbf{t}_c \cdot \delta \mathbf{d} \partial I I^{-1} d\Gamma_{t+\Delta t} \tag{20}$$

where $I = {dS_{t+\Delta t}}/{dS_t}$ and $J = {dV_{t+\Delta t}}/{dV_t}$ represent the ratios between present, $< t + \Delta t >$ and immediately anterior $< t >$ area and volume measures. Rotation between configurations is taken due account with corrotational measures.

The displacement field $\mathbf{d} = \hat{d}(.,t)$, with restriction imposed by contact kinematics, interpolated at element level by functions $\mathbf{N}$ will be written as $\mathbf{d} = \mathbf{N}\mathbf{d}^N$ with $\mathbf{d}^N$ representing the nodal displacements. From it, deformations may be interpolated by means of interpolation matrix $\mathbf{B}_l$ for linear part, and matrix $\mathbf{B}_{nl}$ for the non-linear part, that depends on displacements, $\boldsymbol{\varepsilon} = (\mathbf{B}_l + \mathbf{B}_{nl})\mathbf{d}^N$.

The difference between internal and external virtual work represents an imbalance at the present configuration. After factorizing virtual terms, this imbalance may be computed after Eqs. (15) and (16) as:

$$\delta W_i - \delta W_e = \delta \mathbf{d}^N [\mathbf{F}(\mathbf{d}^N) + \mathbf{F}_c(\mathbf{d}^N)] \tag{21}$$

where, under matrix notation:

$$\mathbf{F} = \int_{V_t} (\mathbf{B}_l + \mathbf{B}_{nl})^T \mathbf{S} dV_t - \int_{V_{t+\Delta t}} \mathbf{N}^T \mathbf{b}\, dV_{t+\Delta t} - \int_{S_{t+\Delta t}} \mathbf{N}^T \mathbf{t}\, dS_{t+\Delta t} \tag{22}$$

Copyright © 2017 ABCM

Vector $\mathbf{F}$, for a given discretization will depend on displacements and hence will require use of an iterative solution scheme. If Newton's method is used (Chapra, 2014), displacement increments $< i, i+1; i = 1,2,..n >$ between sequent iterations will be obtained as:

$$\boldsymbol{\Psi}_i \neq \mathbf{0}; \quad \boldsymbol{\Psi}_{i+1} = \mathbf{0}; \quad \Delta\mathbf{d}_{i,i+1}{}^{N} = -[\partial_{\mathbf{d}}(\boldsymbol{\Psi})]^{-1}\boldsymbol{\Psi}_i; \quad \boldsymbol{\Psi} = \mathbf{F} + \mathbf{F}_c \tag{23}$$

being the gradient of this vector with respect to displacements, also known as Jacobian, given by:

$$\partial_{\mathbf{d}}\mathbf{F} = (\mathbf{K}_l + \mathbf{K}_{nl} + \mathbf{K}_\sigma - \partial_{\mathbf{d}}\mathbf{F}_b - \partial_{\mathbf{d}}\mathbf{F}_t)\partial\mathbf{d}^N \tag{24}$$

with the linear, non-linear and initial stress stiffness matrices, (Zienkiewicz and Taylor, 1989) defined as:

$$\mathbf{K}_l = \int_{V_t} \mathbf{B}_l{}^T \mathbf{C}\mathbf{B}_l dV_t \tag{25}$$

$$\mathbf{K}_{nl} = \int_{V_t} \mathbf{B}_{nl}{}^T \mathbf{C}(\mathbf{B}_l + \mathbf{B}_{nl}) dV_t \tag{26}$$

$$\mathbf{K}_\sigma = \int_{V_t} \mathbf{B}_{nl}{}^T \mathbf{S}\, \partial_{\mathbf{d}}\mathbf{B}_{nl} dV_t \tag{27}$$

being $\mathbf{C}$ a tangent constitutive equation, dependent on the elastic-plastic model. The increments of external body force and applied tractions written as (Abaqus Theory Manual, 2015):

$$\partial_{\mathbf{d}}\mathbf{F}_b = \int_{V_{t+\Delta t}} \mathbf{N}^T \partial\mathbf{b} dV_{t+\Delta t} + \int_{V_{t+\Delta t}} \mathbf{N}^T \mathbf{b}\, \partial_{\mathbf{d}} J\, J^{-1} dV_{t+\Delta t} \tag{28}$$

$$\partial_{\mathbf{d}}\mathbf{F}_t = \int_{S_{t+\Delta t}} \mathbf{N}^T \partial\mathbf{t}\, dS_{t+\Delta t} + \int_{S_{t+\Delta t}} \mathbf{N}^T \mathbf{t}\, \partial_{\mathbf{d}} I\, I^{-1} dS_{t+\Delta t} \tag{29}$$

During processing, the sector of the workpiece in contact with the roll will have contact forces $\mathbf{t}_c = p_n\mathbf{e}_n + \tau_j\mathbf{e}_j; j = 1,2$ local axes, with normal $\partial p_c = k_n \partial d_n$ and tangential $\partial\tau_j = \mathrm{k}_t \partial d_j$ increments in the stick region of contact. Under slip, $\partial\mathbf{d}_c = \partial\mathbf{d}_{ca} + \partial\mathbf{d}_{cs}; \mathbf{d}_c = d_n\mathbf{e}_n + \mathbf{d}_{tj}\mathbf{e}_j$, with the adherent part $\Delta\mathbf{d}_{ca}$ calculated as in stick condition and slip part, $\Delta\mathbf{d}_{cs}$, coming from Coulomb friction condition: $f_c = \sqrt{\tau_x^2 + \tau_y^2} + \mu p_c = 0$, a constraint equation. Once interpolated the interface displacements, the increments of contact forces $\partial\mathbf{F}_c$ will factor an interface matrix $\mathbf{K}_c$, with normal and tangential (Crisfield, 1994) parts as well as linear, non-linear and initial stress components:

$$\mathbf{K}_c = \mathbf{K}_{cl} + \mathbf{K}_{\mathbf{cnl}} + \mathbf{K}_{c\sigma} \tag{30}$$

3. FINITE ELEMENT MODEL

The updated Lagrange formulation, implemented in a commercial finite element package Abaqus™ has been used to analyze a 2D model of a slab of carbon steel processed by cold rolling. A single pass was considered. Dimensions of the strip include the initial length l_0, the width w_0 and the height y_0. Roll, considered rigid, has radius R with rotational velocity ω about axis z. Roll gap confers a reduction $\Delta r = y_i - y_f$ per pass. Feed velocity of the workpiece is designated as v_i. These parameters are listed in the first table below, Tab.1.

Material used in the model is a specific steel, with large applications in the industry that manufactures appliances (Beddoes and Bibbly, 1999). Its most important mechanical properties include the elastic modulus E, Poisson's ratio ν, initial yield strength S_{yo}, density ρ and ultimate strength S_{ut} include in Tab. 2.

Copyright © 2017 ABCM

Table 1 Main parameters of the model

Parameter	*Value*
Length,m	0.100
Width,m	0.050
Roll Radius,m	0.500
Reduction	50%
Roll Speed,rpm	60
Feed Speed,ms^{-1}	1.

Evolution of yield strength with strain hardening is shown in tabular form for points in the working interval of the material in Tab. 3.

Table 2 Mechanical properties of steel AISI 1010 HR

Variable	Value
E, GPa	200.
ν	0.30
ρ, kgm^{-3}	7.85e+3
S_{yt} , MPa	170.
S_{ut} , MPa	380

Table 3. Yield Stress strain data sheet for steel AISI 1010 HR

Yield Stress, MPa	Plastic Strain
174.72	0.0
219.00	0.1
272.00	0.2
308.53	0.3
337.37	0.4
361.58	0.5
382.65	0.6
401.42	0.7
418.42	0.8
434.01	0.9
448.45	1.0

In Fig. 4 it is shown the distribution of von Mises stresses across the workpiece in an intermediate instant of the process – step 1, frame 10/20.

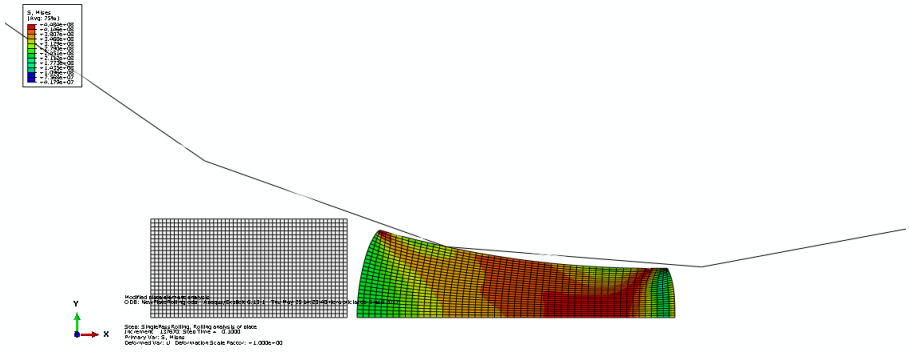

Figure 4 Stress field as measured by Mises stresses at an intermediate position

Copyright © 2017 ABCM

In the situation depicted the left part of the specimen, length *a*, was not processed yet. The central part, length *b* is under the action of the roll, and the righter part, length *c,* has already gotten close to its final height. Stress level at the initial part is in the elastic range, mostly. In the plot undeformed and deformed configurations are shown so as to include the displacement field.

Next plot shows the behavior of the axial stress σ_x. Even though this stress varies in the height direction, this variation is not large – around 10% in a typical section, justifying the analytical simplification. Also, the axial stresses are larger in the interval between the initial contact angle ϕ_i, equal to 18 º, and the neutral n-n position, which occurs at $\phi_n = 5.8^o$.

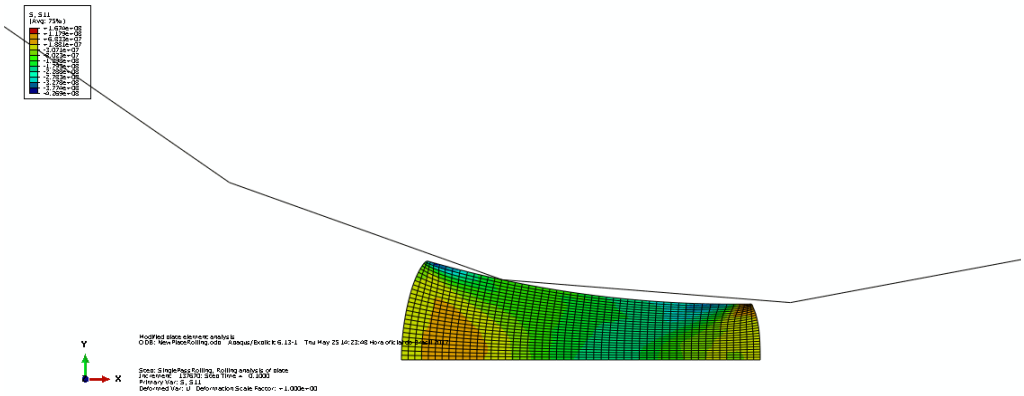

Figure 5 Axial stress distributions along the processing of slab

Presence of shear stresses is expected, at least close to the bite point of the roll, as the distorted form of the slab shows. Figure 6 confirms that this really happens. Not only there, but also along the entrance region. Elements at exit section, with residual strains present, show another confirmation of this fact. Closer to the bite section shear stresses are very large, red color. Residual strains at the exit point are in the 2 up to 5 %.

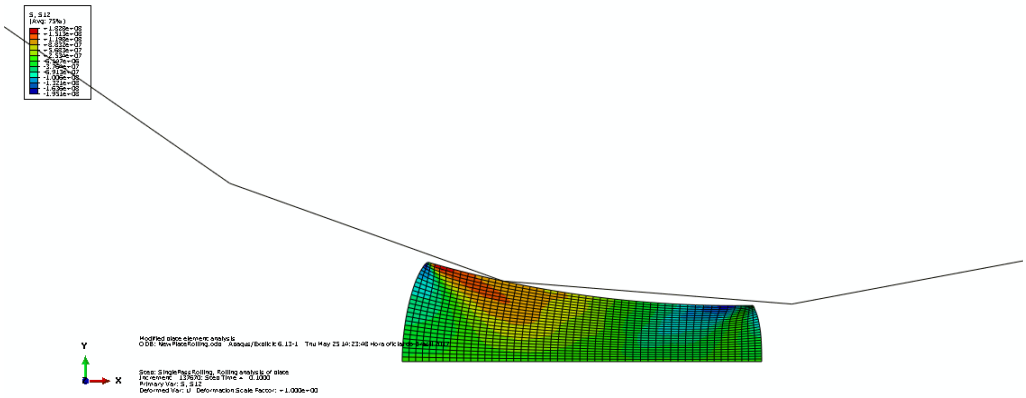

Figure 6 Shear stress distribution in the workpiece

In Fig. 7, the behavior of the vertical stress σ_y along the rolling process is analyzed. Average stress at an element in the half symmetry height line is considered as the element travels from initial up to the exit position. From feed position up to the bite position, i-i section and onwards up to n-n this stress increases continuously. It decreases thereafter up to exit position. Along a vertical line, increases occur as well, by a 10%, in average. This component of stress is much larger than σ_x. The vertical product simplification used in the analytical approach is not confirmed here.

Copyright © 2017 ABCM

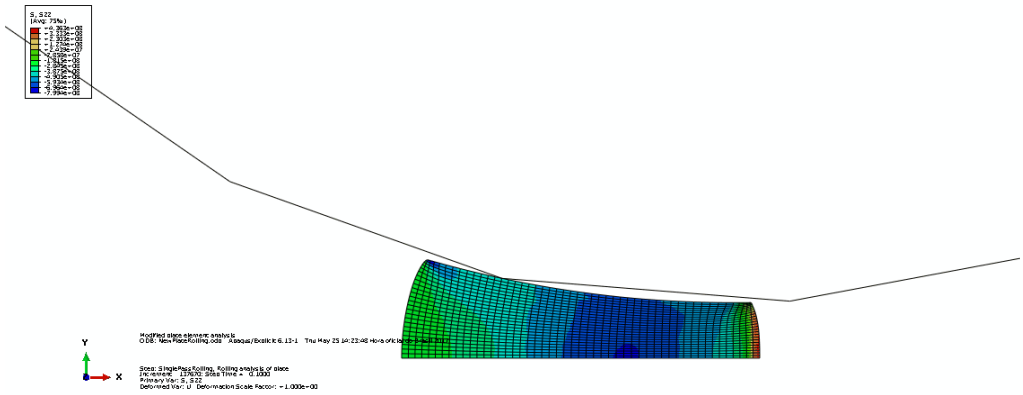

Figure 7 Behavior of vertical stress along the processing zone

Another point worth of verification is the velocity field. If an element at the half height of the slab is followed, from the entry zone, where the magnitude of velocity is the feed velocity up to the exit section, it is seen that: Sections are accelerated as they reach the processing zone and from there on, passing the neutral point faster and leaving last position even faster. Velocity distribution is shown in Fig. 8. Variations of velocity along the x-direction are of the order of 87 % in this study.

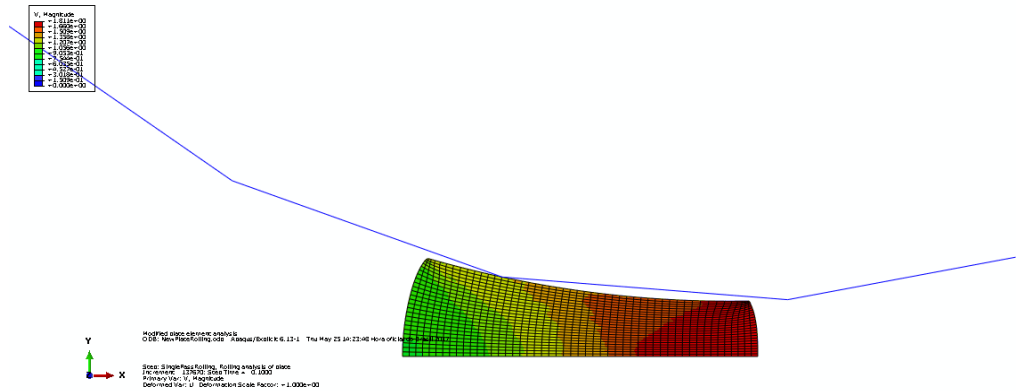

Figure 8 Velocity field across the slab

The contact interaction in the interface between roll and workpiece gives rise to a distribution of normal and tangential contact stresses, Fig. 9 and Fig. 10. Tangential stresses occur after stick limit is passed. Friction depends on the surfaces in contact, their relative velocity and temperature, among others. For Coulomb model, constitutive equations for the interface elements depend on the frictional coefficient μ. Here the average value of 0.4 was taken. Increase of this value would lead to larger roll forces and moments.

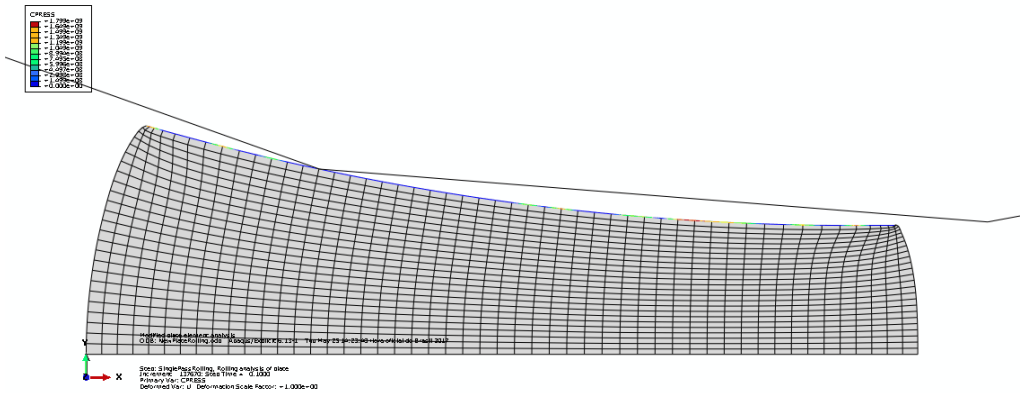

Figure 9 Contact pressure distribution along the upper interface of the model

Copyright © 2017 ABCM

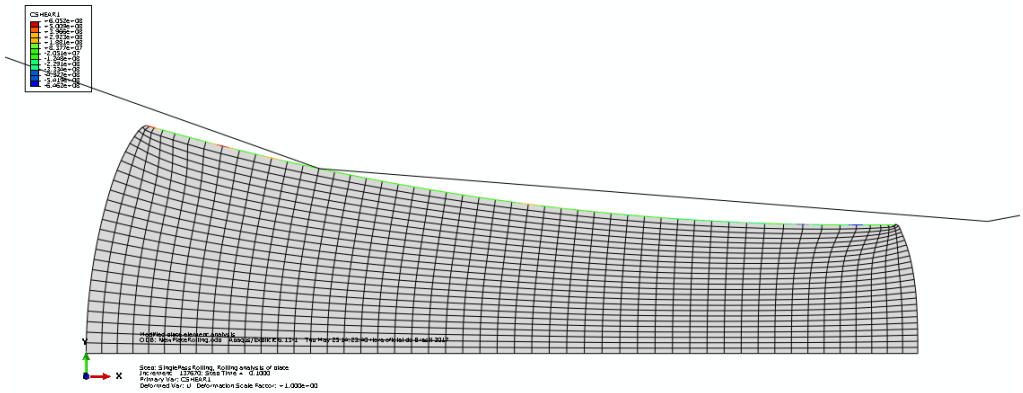

Figure 10. Frictional stresses distribution at the contact elements in the interface

4. COMPARISONS AND CONCLUSIONS

Expressions used in the analytical model have to be taken as a first order approximation to the explaining of the process. The axial field is neither constant nor the shear stresses are null, reason why comparison between numerical and analytical results shows important differences. Finding an improved solution, even numerically, to the differential equation of equilibrium, Eq. (4) would allow lower differences. A Runge-Kutta procedure could be tried. The angle of initial contact used here, much larger than 6º, showed large differences in field values.

The numerical solution presented requires improvement also, as the discretization was poor, mostly in the case of the contact elements. This numerical solution showed the reduction of thickness too large for a single step. The numerical approximation can include strain rate as well as temperature effects in the constitutive behavior of the material. Furthermore, effects of the coefficient of friction on the other parameters of the process can be analyzed. In particular, in the stress distribution that increases with friction, leading to possible failures in the process, an important answer required from a model.

Another problem normally faced by the industry refers to the reduction ratio per pass under different lubrication scenarios. This factor may be considered with the numerical model, as it provides directly the reaction forces in the center of the roll, as well as the required torque to move the workpiece, at every position in the process. And not only in an average sense, can be used to design the rolling equipment.

5. REFERENCES

Kalpakjian, S. et all, 2006, “Manufacturing Engineering and Technology”, 5Th Edition, Pearson Education, USA

Shahani et all, 2009, “Parametric Study of Hot Rolling Process by the Finite Element Method”, Transaction B: Mechanical Engineering, vol. 16, # 2, pp. 130-139

Bathe, K.J., 1996, “Finite Element Procedures”, Prentice Hall Inc., Upper Sadle River, New Jersey, USA

Zienkiewicz, O.C. and Taylor, R.L.,1989, “The Finite Element Method”, McGraw-Hill, New York, USA

Abaqus, 2015, “Theory Manual”, 6.13 Edition, Dassault Systèmes Simulia Corporation, Providence, RI. USA

Dieter, G.E. Jr, 1986, ¨Mechanical Metalurgy”, 3rd. Edition, McGraw-Hill Book. Co., New York, USA

Chapra, 2014, “Numerical Methods for Engineers”, 6Th Edition, McGraw-Hill Book Co., New York, USA

Li. G. and Kobayashi, S., 1982, “Rigid-plastic finite element analysis of plain strain rolling”, Journal of Engineering for Industry, vol. 104, pp. 55-63

Backofen, 1972, “Deformation Processing”, Addison-Wesley, Reading, MA, USA

Belytschko, T.et all, 2000, “Nonlinear Finite Elements for Continua and Structures”, John Wiley, New Jersey, USA

Beddoes, J. and Bibbly, M.J., 1999, “Principles of metal manufacturing process”, Arnold, UK

Crisfield, M.A.,1997, ¨Non-linear Finite Element Analysis of Solids and Structures, vol. II, Advanced Topics, Wiley & Sons

6. RESPONSIBILITY NOTICE

The authors are the only responsible for the printed material included in this paper.